DOI 10.1007/s10812-017-0554-8
Journal of Applied Spectroscopy, Vol. 84, No. 5, November, 2017 (Russian Original Vol. 84, No. 5, September–October, 2017)

AUGER RECOMBINATION AND AMPLIFIED LUMINESCENCE IN InAsSb/InAsSbP LEDS AT 10–60 K

D. M. Kabanau,[a*] **Y. V. Lebiadok,**[a] **and Yu. P. Yakovlev**[b]

UDC 621.315.592;535.37

The Varshni parameters of the temperature dependence of the bandgap energy in the range 10–313 K and the temperature dependence of the spin–orbit splitting energy have been calculated using experimental data obtained for an $InAs_{0.88}Sb_{0.12}$ active layer. Amplified luminescence was observed in the range 10–35 K for LEDs based on $InAs_{0.88}Sb_{0.12}$/InAsSbP heterostructures. The sharp drop in radiation intensity of InAsSb/InAsSbP LEDs at temperatures >32 K was due to extensive growth of the CHCC Auger-recombination process while the CHSH process was the dominant Auger-recombination process at temperatures <35 K.

Keywords: *InAsSb, amplified luminescence, Auger recombination, internal quantum yield of luminescence.*

Introduction. Optoelectronic devices based on InAsSb/InAsSbP light-emitting diodes (LEDs) are widely used for environmental monitoring and industrial process control, in medicine and other sectors [1–3], and for scientific research within and without space laboratories and satellites [4]. The spectral and energy characteristics of semiconductor structures near room temperature [5, 6] and at cryogenic temperatures [7, 8] must be known in detail to apply mid-IR-range LEDs in these areas. Several physical processes occurring in the emitting active layers of InAsSb/InAsSbP heterostructures are insufficiently studied and require further research. In particular, Auger recombination is known to be the main quenching process in narrow-band semiconductors [7]. However, this process for InAsSb/InAsSbP LEDs has not been studied in detail. Also, the temperature dependences of the bandgap and spin–orbit splitting of the band for InAsSb solid solutions are poorly understood.

The present work investigated amplified luminescence and Auger recombination in InAsSb/InAsSbP LEDs and estimated the temperature dependence of the bandgap of $InAs_{0.88}Sb_{0.12}$ solid solution.

Experimental. LEDs based on InAsSb/InAsSbP heterostructures were investigated experimentally. Their luminescence spectrum maxima at room temperature were situated near 4.3 μm. The LED chips were squares with sides of 400 μm and surfaces with Ohmic ring contacts of external diameter 350 μm and width 15 μm that were mounted by the substrate side to a TO-18 body.

The heterostructures of the studied LEDs were grown on *n*-InAs substrate in (100) orientation that was doped with Sn to a carrier concentration of $5 \cdot 10^{18}$ cm^{-3}. The fundamental absorption edge of a substrate with such a high carrier concentration was shifted to shorter wavelength so that it became transparent for radiation of wavelength $\lambda \geq 2.5$ μm. A buffer layer of *n*-$InAs_{0.94}Sb_{0.06}$ 3.3 μm thick was grown by liquid-phase epitaxy on the substrate to decrease deformation of the active region. Then, a broad-band emitting layer of *n*-$InAs_{0.50}Sb_{0.20}P_{0.30}$ 6.2 μm thick that was doped with Sn to a concentration of ~$5 \cdot 10^{17}$ electrons/cm^{-3}, an undoped ($n \sim 5 \cdot 10^{15}$ cm^{-3}) active layer of *n*-$InAs_{0.88}Sb_{0.12}$ 2.5 μm thick, and a broad-band emitting layer of *p*-$InAs_{0.50}Sb_{0.20}P_{0.30}$ 1.4 μm thick doped with Zn to a concentration of $2 \cdot 10^{18}$ holes/cm^{-3} were grown. Then, the substrate was ground to a thickness of 200 μm and polished. Ohmic contacts were formed by thermal vacuum sputtering of Cr/Au–Te/Au layers to the *n*-InAs substrate and Cr/Au–Ge/Au layers to the *p*-layer [3].

The LEDs were placed into a vacuum cryostat with a sapphire output window. The contacts from the LED were hermetically fed to the outside of the cryostat. The cooling system could change and control the temperature in the range 10–60 K. The LED was supplied with power in pulse mode (50% quasi-continuous mode) at pulse rate 16 kHz and injection current 208 mA.

[*]To whom correspondence should be addressed.

[a]SSPA Optics, Optoelectronics & Laser Technology, National Academy of Sciences of Belarus, 68 Nezavisimost′ Ave., Minsk, 220072, Belarus; email: d.kabanau@ifanbel.bas-net.by; [b]Ioffe Physical-Technical Institute, Russian Academy of Sciences, St. Petersburg, Russia. Translated from Zhurnal Prikladnoi Spektroskopii, Vol. 84, No. 5, pp. 786–793, September–October, 2017. Original article submitted March 27, 2017.

0021-9037/17/8405-0843 ©2017 Springer Science+Business Media New York

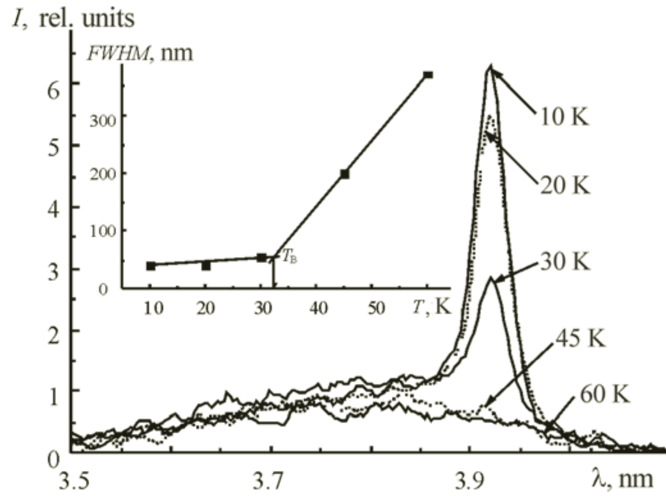

Fig. 1. Temperature dependence of LED emission spectrum with $InAs_{0.88}Sb_{0.12}$ active region with current 208 mA; in the inset, temperature dependence of emission spectrum full width at half-maximum (*FWHM*), T_B = 32 K is the temperature below which the spectrum narrows sharply.

TABLE 1. Energy Parameters of $InAs_{0.88}Sb_{0.12}$ Solid Solution

$\Delta_{so}(0)$, meV	χ, eV/K	m_{so}/m_0	$E_g(0)$, meV	α, eV/K	β, K
308.5	$0.81 \cdot 10^{-4}$	0.35	312.0	$3.863 \cdot 10^{-4}$	194.99

Spectra were recorded using an MS2004i monochromator spectrometer (SOL Instruments) with resolving power of at least 3 nm in this spectral range. LED emission was detected using an HgCdTe photomultiplier with automated sensitivity correction in the range 1–5 μm. Figure 1 shows experimental LED luminescence spectra with an $InAs_{0.88}Sb_{0.12}$ active region.

Temperature Dependence of $InAs_{0.88}Sb_{0.12}$ Bandgap Width. The temperature dependence of the bandgap width of an LED with an $InAs_{0.88}Sb_{0.12}$ active region was estimated by plotting the temperature dependence of the long-wavelength edge of the experimental spectra (the position of the edge was determined from the intersection of the tangent to the luminescence-spectrum long-wavelength edge at zero intensity). The resulting experimental temperature dependences of the bandgap widths at 10–60 K for the studied structures were approximated by the Varshni formula [9]:

$$E_g(T) = E_g(0) - \alpha T^2/(\beta + T)\,, \tag{1}$$

where $E_g(0)$ is the bandgap width at 0 K; α and β, Varshni parameters. The approximating curve for the studied structure deviated by ≤0.15% from the experimental temperature dependence of the bandgap width determined by the Varshni formula. The temperature dependence of the $InAs_{0.88}Sb_{0.12}$ bandgap width in the range 80–313 K was reported before [3]. Table 1 presents combined results obtained in this work and before [3] and those approximated by Eq. (1) in the range 10–313 K with the Varshni parameters given therein. Figure 2a shows the approximated temperature dependence of the bandgap width for $InAs_{0.88}Sb_{0.12}$ in the range 10–313 K (considering the previous results [3]). The Varshni parameters given in Table 1 and the literature [3] differed because the approximation [3] covered a rather linear portion of the dependence of the bandgap width in the range 80–313 K whereas it was nonlinear at low temperatures. Thus, the approximation over the broad temperature range 10–313 K was more correct and accurate.

Auger recombination in $InAs_{0.88}Sb_{0.12}$/InAsSbP LED. Studies of the temperature dependence of the integrated luminescence intensity of semiconductor LEDs could find the thermal luminescence quenching parameters and establish the main processes responsible for nonradiative recombination in the LED active region. The activation energy of thermal luminescence quenching was calculated by plotting the experimental temperature dependence of the integrated emission intensity [10, 11]. Figure 2b shows the experimental dependence of the integrated emission intensity of $InAs_{0.88}Sb_{0.12}$/InAsSbP LED on inverse temperature.

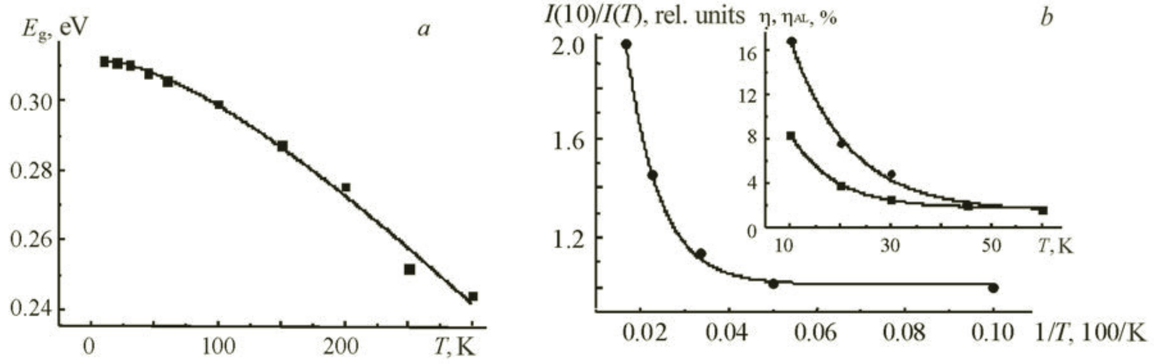

Fig. 2. Dependence of $InAs_{0.88}Sb_{0.12}$ bandgap width on temperature (a) and dependence of integrated LED emission intensity on inverse temperature (b); in the inset, dependence of $InAs_{0.88}Sb_{0.12}$ LED internal quantum yield η and η_{AL} on temperature.

The main processes of Auger recombination that are caused by thermal luminescence quenching in narrow-band semiconductors are CHSH (in which recombination energy of the electron–hole pair is transferred to a hole with a transition of the latter into a spin–orbit split band) and CHCC (involving two electrons and a heavy hole and excitation of an electron into a higher-energy state) [7, 12, 13]. Shockley–Reed–Hall recombination for these LEDs can be neglected for injection current >100 mA [14]. Therefore, thermal luminescence quenching for $InAs_{0.88}Sb_{0.12}/InAsSbP$ could be written as the Arrhenius–Mott formula for the two quenching processes [10, 11]:

$$I(T) = I(0)/1 + Z_1 \exp(-E_{CHSH}/kT) + Z_2 \exp(-E_{CHCC}/kT)\,, \tag{2}$$

where $I(T)$ is the integrated luminescence intensity at temperature T; $I(0)$, integrated luminescence intensity at $T = 0$ K; Z_1 and Z_2, quenching constants for each of the channels of this structure; k, Boltzmann′s constant; E_{CHSH} and E_{CHCC}, activation energies of the CHSH and CHCC processes that were determined from the formulas [15, 16]:

$$E_{CHSH}(T) = (2m_v + m_c)(E_g(T) - \Delta_{so}(T))/(2m_v + m_c - m_{so})\,,$$

$$E_{CHCC}(T) = m_c E_g(T)/(m_v + m_c)\,, \tag{3}$$

where $\Delta_{so}(T)$ is the spin–orbit splitting energy; m_{so}, m_c, and m_v, effective masses of carriers in a spin–orbit split band, electrons in the conductivity band, and heavy holes, respectively. The temperature dependence of the band spin–orbit splitting energy for crystals of similar structures and solid solutions was written [17]:

$$\Delta_{so}(T) = \Delta(0) + \chi T\,, \tag{4}$$

where $\Delta(0)$ is the band spin–orbit splitting energy at $T = 0$ K and χ, the linear temperature dependence parameter.

The quantities $\Delta_{so}(0)$, χ, and m_{so} could be determined by comparing the experimental temperature dependence of the LED integrated emission intensity with those calculated using Eqs. (2)–(4). Their values were determined by fitting the calculated and experimental curves until they agreed. Figure 2b shows the curve for the best approximation of the experimental data. Parameters m_c and m_v from the literature [18] (the temperature dependence of the effective masses was rather small) and the dependence of the experimental bandgap width (Varshni formula and parameters from Table 1) were used in the calculations for $InAs_{0.88}Sb_{0.12}$. Table 1 presents the $\Delta_{so}(0)$, χ, and m_{so} values obtained from the experimental data.

The function $E_{CHSH}(T)$ in Eq. (3) was only valid for $E_g(T) > \Delta_{so}(T)$ [13, 15]. Thus, $\Delta_{so}(T)$ could be obtained experimentally to temperatures at which $E_g(T) = \Delta_{so}(T)$.

Figure 1 shows that the temperature dependence of the *FWHM* of the emission spectrum had a break at 32 K for solid solutions $InAs_{0.88}Sb_{0.12}$ and that the emission intensity decreased. Amplified luminescence that disappeared at higher temperatures was observed at $T < 32$ K for $InAs_{0.88}Sb_{0.12}/InAsSbP$ LEDs. Experimental temperature dependences of E_g and Δ_{so} (extrapolated to a larger temperature range) and the following equations [19, 20, 21] were used to establish that Auger recombination leading to luminescence quenching was dominant:

$$C_{CHCC}(T) = \frac{\pi^{1/2}}{2\hbar}\,\frac{m_c(m_c + m_v)^2}{(2m_v + m_c)}\left|M_{ee}^2\right|\frac{E_{CHCC}(T)^2}{(kT)^{3/2}}\exp\left(\frac{-E_{CHCC}(T)}{kT}\right), \tag{5}$$

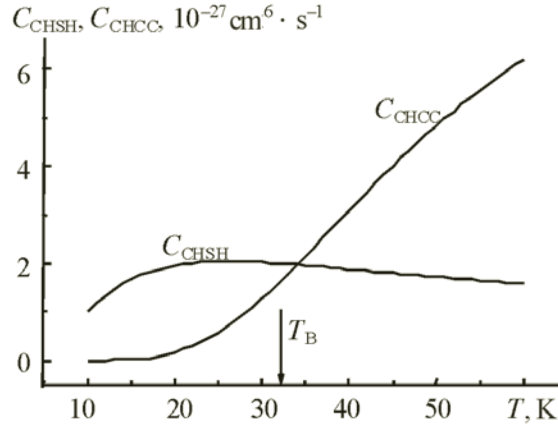

Fig. 3. Temperature dependence of Auger recombination for $InAs_{0.88}Sb_{0.12}$/InAsSbP LED.

$$\begin{cases} C_{CHSH} = ABx^2e^x \dfrac{2}{\pi^{1/2}} \left(\Gamma(3/2, \mu x) - \dfrac{2\Gamma(5/2, \mu x)}{\mu x} + \dfrac{\Gamma(7/2, \mu x)}{\mu^2 x^2}\right), \quad E_g \geq \Delta, \\ C_{CHSH} = ABx^2e^x \left(1 - \dfrac{3}{\mu x} + \dfrac{15}{4\mu^2 x^2}\right), \quad E_g \leq \Delta, \\ A = \dfrac{g(\varepsilon)\pi^3\hbar^3 e^4}{2m_0^2}\left(\dfrac{m_v}{m_h}\right)^3 \left(\dfrac{m_{so}}{2m_v + m_c}\right)^{3/2}, \quad B = \dfrac{(|M_{ee}^2|2/m_0)^2(1 + m_{so}/m_0)}{9E_g^2\Delta^2(E_g + \Delta)}, \\ x = \dfrac{E_g - \Delta}{k_B T}, \quad \mu = \dfrac{2m_v + m_c}{2m_v + m_c - m_{so}}, \end{cases} \tag{6}$$

where $\Gamma(a, x_0) = \int_{x_0}^{\infty} e^{-t}t^{a-1}dt$; $g(\varepsilon)$ is a shielding function; m_0, free electron mass; and $|M_{ee}|^2$, the square of the matrix element. The parameters for the calculations were taken from the literature [22, 23].

The band spin–orbit splitting energy for solid solution $InAs_{0.88}Sb_{0.12}$ was 308.6 meV as calculated from Eq. (4) and extrapolated to 77 K using the parameters in Table 1. This agreed satisfactorily with the experimental data for $InAs_{0.91}Sb_{0.09}$ at 77 K (Δ_{so} = 325 meV) [18].

Figure 3 shows temperature dependences of the CHSH and CHCC processes that were calculated using Eqs. (5) and (6). It can be seen that Auger-recombination CHSH began to develop strongly as the temperature rose to 27 K, after which the energy difference between $E_g(T)$ and $\Delta_{so}(T)$ increased. This led to a smooth decrease of the Auger-recombination CHSH coefficient. The CHCC process developed strongly as the environmental temperature increased to >20 K. Thus, the results established that Auger-recombination CHSH limited the luminescence intensity at low temperatures (0–30 K) for $InAs_{0.88}Sb_{0.12}$. Also, the CHCC process increased exponentially as the temperature increased to >20 K and began to dominate over CHSH at >35 K. This led to general luminescence quenching at temperatures >32 K.

Amplified Luminescence in $InAs_{0.88}Sb_{0.12}$/InAsSbP LEDs. Figure 1 shows that the luminescence spectrum narrowed sharply near temperature T_B as the temperature decreased from 60 to 10 K. Luminescence amplification in $InAs_{0.88}Sb_{0.12}$/InAsSbP LEDs was studied in detail by calculating emission spectra and amplification coefficient $g(E)$ using a model for optical interband transitions without selection rules for the electron wave vector. The modeling was based on the system of equations [24–26]:

$$W_{sp}(E) = \frac{2e^2 r_0 |\mathbf{M}|^2}{\pi^5 \varepsilon_0 \hbar^8 c^3} m_c^{3/2} m_v^{3/2} E^2 \int_{E_g}^{E} \sqrt{(E_c - E_g)(E - E_c)} f_e(E_c) f_h(E_c - E) dE_c,$$

$$g(E) = \frac{1}{W_{sp}(E)} \frac{\pi^2 c^2 \hbar^3}{r_0^2 E^3}\left(1 - \exp\frac{E - \Delta F}{kT}\right), \quad S_{AL}(E) = \frac{W_{sp}(E)}{K_{AL} - \tilde{A}g(E)}, \tag{7}$$

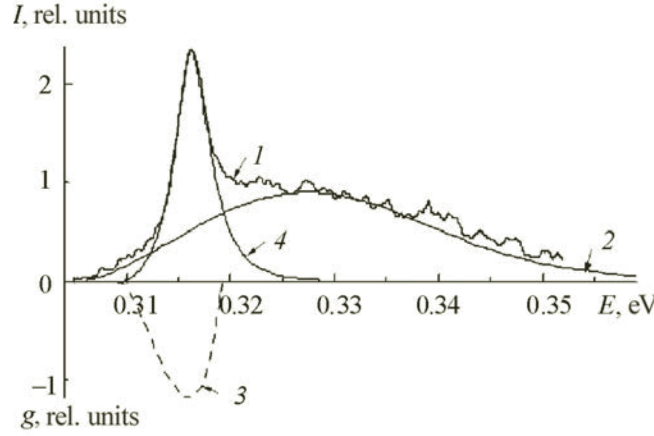

Fig. 4. Comparison of experimental and calculated $InAs_{0.88}Sb_{0.12}$/InAsSbP LED luminescence spectra at 30 K: experimental spectrum (1), calculated luminescence spectral power $W_{sp}(E)$ (2), amplification coefficient $g(E)$ (3), and calculated amplified luminescence spectrum $S_{AL}(E)$.

where $W_{sp}(E)$ is the spontaneous luminescence spectral power; E, photon energy; r_0, InAsSb index of refraction; e, electron charge; $|M|^2$, square of optical interband transition matrix element average over space and polarization; ε_0, electrical constant; c, speed of light in a vacuum; E_c, conductivity-band state energy (the top of the valence band $E_{v0} = 0$ was taken as the calculation origin; the bottom of the conductivity band energy $E_{c0} = E_g$); $f_e(E)$ and $f_h(E)$, Fermi–Dirac functions for electrons and holes with energy E; F_e and F_h, positions of Fermi quasi-levels in the conductivity and valence bands; k_B, Boltzmann′s constant; $S_{AL}(E)$, amplified luminescence spectral density; Γ, optical limitation factor; and K_{AL}, amplified luminescence loss coefficient. Quantities F_e and F_h were determined by solving the electroneutrality equation for a degenerate semiconductor with equal concentrations of electrons and holes considering that $\Delta F = F_e - F_h$, where ΔF is the difference of Fermi quasi-levels. All parameters with the exception of the fitting ones were taken from the literature [18, 27, 28].

Parameters ΔF and K_{AL} were fit to construct theoretical luminescence $W_{sp}(E)$ and amplified luminescence spectra $S_{AL}(E)$, calculated using Eqs. (7), and normalized to unity. Figure 4 shows the results. The fitting included adjusting the calculated spectra to the shape of the recorded emission spectra. The experimental spectrum could not be represented as a single luminescence spectrum $W_{sp}(E)$ for all physically possible values of ΔF. The experimental $InAs_{0.88}Sb_{0.12}$/InAsSbP LED emission spectrum was described best by the luminescence spectrum calculated considering the amplified luminescence spectrum. Figure 4 shows that a strong experimental emission maximum was located in the region of a positive amplification coefficient, thereby confirming the hypothesis that amplified luminescence was observed at low temperatures (10–40 K) in $InAs_{0.88}Sb_{0.12}$ LEDs.

The fitting parameters found using this method were used to find the absolute value of the emission spectral density $r_{sp}(E) = W_{sp}(E)/E$ and the emission induced by amplified luminescence. The resulting values of $r_{sp}(E)$ and $S_{AL}(E)$ ultimately enabled the internal quantum yield to be estimated considering and not considering amplified luminescence in the range 10–60 K. For this, the rates of radiative and nonradiative recombination of solid solution $InAs_{0.88}Sb_{0.12}$ were calculated at various temperatures.

The rate of radiative recombination R_{SE} was calculated using the formula [26]:

$$R_{SE} = \int_{\Delta E} r_{sp}(E)dE, \tag{8}$$

where ΔE is the spectral band in which luminescence was observed. The rate of recombination induced by amplified luminescence was determined using the formula [26]:

$$R_{AL} = \frac{1}{E} \int_{\Delta E_u} g(E) S_{AL}(E)dE, \tag{9}$$

where ΔE_u is the spectral band in which the amplification coefficient was non-negative. The rate of nonradiative recombination Q was estimated from the equation [25]:

TABLE 2. Recombination Rate Parameters at Various Temperatures for $InAs_{0.88}Sb_{0.12}/InAsSbP$ LEDs

Temperature, K	R_{SE}, 10^{28} s^{-1}·m^{-3}	R_{AL}, 10^{27} s^{-1}·m^{-3}	Q, 10^{29} s^{-1}·m^{-3}
10	0.333	4.802	0.362
20	1.754	18.977	4.371
30	3.052	23.396	10.567
45	6.162	14.015	29.531
60	10.014	10.369	61.269

$$j = ed(R_{SE} + Q + R_{AL}) , \qquad (10)$$

where d is the active layer thickness and j, the experimental injection current density.

Table 2 gives the rates of radiative and nonradiative recombination and recombination induced by amplified luminescence that were calculated from Eqs. (8)–(10) and were used to estimate the luminescence internal quantum yield $\eta = R_{SE}/(R_{SE} + Q)$ and the quantity $\eta_{AL} = (R_{SE} + R_{AL})/(R_{SE} + R_{AL} + Q)$, which considered the effect of amplified luminescence. Figure 2b (inset) shows the temperature dependences of these quantities.

The loss coefficient of amplified luminescence K_{AL} for $InAs_{0.88}Sb_{0.12}$ LED was 8–9 cm^{-1} in the temperature range 10–60 K, which was close to the literature value [8]. The amplified luminescence loss coefficient was shown to obey the expression [26]:

$$\Delta = K_{AL}\sqrt{S} , \qquad (11)$$

where S is the area of the p–n-transition and Δ, a proportionality coefficient that was 0.08 for the studied LED.

The resulting values R_{SE}, R_{AL}, and Q allowed the fraction of amplified luminescence in the total emission of the InAsSb/InAsSbP structures to be calculated. The fraction increased with decreasing temperature for these LEDs. Thus, the calculated fraction of amplified luminescence in the total emission of heterostructure $InAs_{0.88}Sb_{0.12}/InAsSbP$ LEDs decreased from 60 to 10% as the temperature changed from 10 to 60 K.

Conclusions. Varshni parameters and spin–orbit splittings of bands for $InAs_{0.88}Sb_{0.12}$ solid solutions in the range 10–313 K were obtained from the experimental temperature dependences of $InAs_{0.88}Sb_{0.12}/InAsSbP$ LEDs. It was found that Auger recombination CHSH was the process limiting the luminescence intensity of $InAs_{0.88}Sb_{0.12}$ structures at low temperatures (10–30 K). The CHCC process grew exponentially as the temperature increased to >20 K and started to dominate over the CHSH process at $T > 35$ K. This led to general luminescence quenching. It was shown that InAsSb/InAsSbP LED luminescence spectra at low temperatures agreed with the optical interband transition model without selection rules for the electron wave vector considering the effect of amplified luminescence. The modeling enabled the temperature dependence of the internal quantum yield for this structure to be calculated. The internal quantum yield for $InAs_{0.88}Sb_{0.12}$ structures decreased by an order of magnitude as the temperature increased from 10 to 60 K. The fraction of amplified luminescence in the total emission from this type of LED decreased from 60 to 10% as the temperature increased in this range.

Acknowledgments. We thank N. V. Rzheutskii for assistance with performing the experiments.

REFERENCES

1. A. S. Golovin, A. A. Petukhov, S. S. Kizhaev, and Yu. P. Yakovlev, *Pis'ma Zh. Tekh. Fiz.*, **37**, No. 11, 15–19 (2011).
2. H. T. Whelan, E. V. Buchmann, N. T. Whelan, S. G. Turner, V. Cevenini, H. Stinson, R. Ignatius, T. Martin, J. Cwiklinski, G. A. Meyer, B. Hodgson, L. Gould, M. Kane, G. Chen, and J. Caviness, in: *Space Technology and Applications International Forum-2001*, CP552, American Institute of Physics, (2001), pp. 35–45.
3. T. V. Bez'yazychnaya, M. V. Bogdanovich, V. V. Kabanov, D. M. Kabanov, E. V. Lebedok, V. V. Parashchuk, A. G. Ryabtsev, G. I. Ryabtsev, P. V. Shpak, M. A. Shchemelev, I. A. Andreev, E. V. Kunitsyna, V. V. Sherstnev, and Yu. P. Yakovlev, *Fiz. Tekh. Poluprovodn.*, **49**, No. 7, 1003–1006 (2015).
4. W. Lu, T. Zhang, S. M. He, B. Zhang, N. Li, and S. S. Liu, *Opt. Quantum Electron.*, **41**, 883–893 (2009).
5. V. G. Harutyunyan, K. M. Gambaryan, V. M. Aroutiounian, and I. G. Harutyunyan, *Infrared Phys. Technol.*, **70**, 12–14 (2015).
6. Sanjeev and P. Chakrabarti, *Infrared Phys. Technol.*, **67**, 382–386 (2014).

7. K. D. Mynbaev, N. L. Bazhenov, A. A. Semakov, M. P. Mikhailova, N. D. Stoyanov, S. S. Kizhaev, S. S. Molchanov, A. P. Astakhova, A. V. Chernyaev, H. Lipsanen, and V. E. Bugrov, *Fiz. Tekh. Poluprovodn.*, **51**, No. 2, 247–252 (2017).
8. A. P. Astakhova, T. V. Bezʹyazychnaya, L. I. Burov, A. S. Gorbatsevich, A. G. Ryabtsev, G. I. Ryabtsev, M. A. Shchemelev, and Yu. P. Yakovlev, *Fiz. Tekh. Poluprovodn.*, **42**, No. 2, 228–231 (2008).
9. I. A. Vainshtein, A. F. Zatsepin, and V. S. Kortov, *Fiz. Tverd. Tela*, **41**, No. 6, 994–998 (1999).
10. V. G. Talalaev, B. V. Novikov, G. E. Tsyrklin, and H. S. Leipner, *Fiz. Tekh. Poluprovodn.*, **49**, No. 11, 1531–1539 (2015).
11. D. G. Chtchekine, G. D. Gilliland, Z. C. Feng, S. J. Chua, D. J. Wolford, S. E. Ralph, M. J. Schurman, and I. Ferguson, *MRS J. Nitride Semicond. Res. 4S1*, G6.47 (1999).
12. M. Leroux, N. Grandjean, B. Beaumont, G. Nataf, F. Semond, J. Massies, and P. Gibart, *J. Appl. Phys.*, **86**, 3721 (1999).
13. K. J. Cheetham, A. Krier, I. P. Marko, A. Aldukhayel, and S. J. Sweeney, *Appl. Phys. Lett.*, **99**, 141110 (2011).
14. A. A. Petukhov, B. E. Zhurtanov, S. S. Molchanov, N. D. Stoyanov, and Yu. P. Yakovlev, *Zh. Tekh. Fiz.*, **81**, No. 4, 91–96 (2011).
15. M. Takeshima, *Phys. Rev. B: Condens. Matter Mater. Phys.*, **26-2**, 917–930 (1982).
16. M. Takeshima, *J. Appl. Phys.*, **43**, 4114 (1972).
17. M. Takeshima, *Phys. Rev. B: Condens. Matter Mater. Phys.*, **25-8**, 5390–5414 (1982).
18. I. Vurgaftman and J. R. Meyer, *Appl. Phys. Rev.*, **89**, 5815–5875 (2001).
19. A. Haug, *J. Phys. C: Solid State Phys.*, **17**, 6191–6197 (1984).
20. C. R. Pidgeon, C. M. Ciesla, and B. N. Murdin, *Prog. Quantum Electron.*, **21-5**, 361–419 (1998).
21. A. Haug, *J. Phys. Chem. Solids*, **49-6**, 599–605 (1988).
22. http://www.ioffe.ru/SVA/NSM/Semicond/InAsSb
23. Landolt-Börnstein, *Numerical Data and Functional Relationships in Science and Technology. Group III: Condensed Matter. Vol. 44 Semiconductors, Subvolume C. New Data and Updates for III–V, II–VI, and I–VII Compounds*, U. Roessler (Ed.), Springer-Verlag Heidelberg, Berlin (2010).
24. P. T. Landsberg, M. S. Abrahams, and M. Osinski, *IEEE J. Quantum Electron.*, **QE-21**, 24 (1985).
25. A. A. Afonenko, V. K. Kononenko, I. S. Manak, and V. A. Shevtsov, *Fiz. Tekh. Poluprovodn.*, **31**, No. 9, 1087–1091 (1997).
26. V. P. Gribkovskii, *Theory of Light Absorption and Emission in Semiconductors* [in Russian], Nauka i Tekhnika, Minsk (1975).
27. M. S. Bresler, M. Levinshtein, S. Rumyantsev, and M. Shur, *Handbook Series on Semiconductor Parameters*, World Scientific, London (1999), Vol. 2, pp. 132–152.
28. A. Miller, in: *Nonlinear Optics in Semiconductors II*, E. Garmire, and A. Kost (eds.), *Semiconductors and Semimetals*, Vol. 59, Academic, New York, (1999), 287 p.